Processing and Application of Ceramics 18 [1] (2024) 117–122
https://doi.org/10.2298/PAC2401117K

Microstructure, dielectric and ferroelectric properties of $CaCu_{3-x}Zn_xTi_{4-x}Ce_xO_{12}$ ceramics prepared via semi-wet route

Anuj Kumar Gond[1], Atendra Kumar[2], Anees A. Ansari[3], Sunil Kumar[4], Sumit Kumar[5], Ajit N. Gupta[6], Akhilesh Kumar[7], Youngil Lee[8], Kamdeo Mandal[9,*], Himanshu Shekher[1,*], Laxman Singh[10,*]

[1]*Department of Chemistry, Veer Kunwar Singh University, Ara, Bihar-802301, India*
[2]*Department of Chemistry, Simdega College (Ranchi University), Simdega-835223, Jharkhand, India*
[3]*College of Science, King Saud University, Riyadh, 11451, Kingdom of Saudi Arabia*
[4]*Department of Chemistry, L.N.T. College, B.R.A. Bihar University, Muzaffarpur-842002, Bihar, India*
[5]*Department of Chemistry, Magadh University, Bodhgaya-824234, Bihar, India*
[6]*Department of Chemistry, Govt. (P.G.) College, Charkhari, Mahoba-210421, U.P., India*
[7]*Department of Zoology, (Patna Science College) Patna University, Patna, Bihar-800004, India*
[8]*Department of Chemistry, University of Ulsan, 93 Deahak-ro, Nam-Gu, Ulsan 44610, Republic of Korea*
[9]*Department of Chemistry, Indian Institute of Technology, BHU, Varanasi-221005, U.P., India*
[10]*Department of Chemistry, Siddharth University, Kapilvastu, Siddharth Nagar-272202, U.P., India*

Received 25 May 2023; Received in revised form 18 December 2023; Received in revised form 25 February 2024; Accepted 25 March 2024

Abstract

In this work, the effect of bi-substitution of Zn and Ce at Cu and Ti sites on microstructure and dielectric properties of $CaCu_3Ti_4O_{12}$ ceramics was investigated. The doped $CaCu_{3-x}Zn_xTi_{4-x}Ce_xO_{12}$ (CCZTC-x) powders (where x = 0.1, 0.2 and 0.3) were successfully synthesized via semi-wet route and the corresponding ceramics were obtained by sintering at 950 °C for 14 h in air. The presence of major cubic $CaCu_3Ti_4O_{12}$ phase along with minor secondary CuO phase was observed by X-ray diffraction analysis. Scanning electron microscopy analyses confirmed microstructure consisting of cubic-shaped grains and grain sizes of 0.76, 0.87 and 0.98 μm, for the ceramics with x = 0.1, 0.2 and 0.3, respectively. The high value of relative dielectric constant of 1500 at 100 Hz was found for the sample with x = 0.3, which may be regarded as having semiconducting grains surrounded by insulating grain boundaries. In addition, conductivity of the sintered samples decreases with doping concentrations and the activation energies of the samples with x = 0.1, 0.2 and 0.3 are 0.93, 0.76 and 0.74 eV, respectively.

Keywords: *doped $CaCu_3Ti_4O_{12}$, co-substitution, semi-wet route, microstructure, dielectric properties*

I. Introduction

The high dielectric constant (10^3–10^5) at room temperature in the frequency region of 10^2–10^4 is characteristic of $ACu_3Ti_4O_{12}$ (A = Cd, Ca, $K_{1/2}La_{1/2}$, $Li_{1/2}La_{1/2}$) ceramics with perovskite-like structure [1,2]. The high dielectric constant of single crystal and polycrystalline $CaCu_3Ti_4O_{12}$ (CCTO) ceramics mainly arises from the larger difference in resistance of grain and grain boundaries which is governed by internal barrier layer capacitance (IBLC) mechanism. According to IBLC mechanism, CCTO ceramics can be regarded as inhomogeneous system consisting of semiconducting grains surrounded by insulating grain boundaries, so that maximum charge accumulation occurs at grain boundaries. CCTO ceramics have a good thermal stability in the temperature range of 100–400 K without any structural

*Corresponding author: tel: +91 5544297153
e-mail: *hshe2503@rediffmail.com* (H. Shekher)
kdmandal.apc@itbhu.ac.in (K.D. Mandal)
laxmanresearcher@suksn.edu.in (L. Singh)

change [3–6]. The creation of large amount of oxygen vacancies inside the grains during the cooling process, the reduction of Cu^{2+} ions into Cu^{+} at higher temperature as well as other factors are responsible for different electrical properties of CCTO ceramics [7,8].

The various preparation methods such as sol-gel [9,10], wet chemical method [11], solid state reaction [12], auto combustion method [13] and spark plasma sintering [14], have been employed for the fabrication of $CaCu_3Ti_4O_{12}$ ceramics. The physical properties such as morphology, phase purity and particle size were controlled by synthesis method of $CaCu_3Ti_4O_{12}$ ceramics applicable in various applications like microwave devices, electroceramics, memory device, electronic, gas sensor and varistors [15,16]. From many earlier studies, it was observed that the effect of sintering time and temperature increases the grain size and aggregation of Cu rich phases at the grain boundaries which efficiently affect the microstructure as well as dielectric properties of perovskite-type CCTO ceramics [17–19]. In spite of this, the change of microstructure and dielectric properties could also be obtained by doping other elements in the host materials [20–22]. Most of the work has been reported for improvement of dielectric permittivity and reduction in $\tan\delta$ value with incorporation of dopants at Cu or Ti sites in the CCTO ceramics. The dielectric permittivity of $CaCu_3Ti_4O_{12}$ ceramics was boosted by partial isovalent ion substitution of Zn or Mg on the Cu site because this altered the mixed-valence structure. Under these conditions, the higher dielectric response in CCTO ceramics may be related to the Ti^{3+}/Ti^{4+} ratio, rather than the modest change in the Cu^{+}/Cu^{2+} ratio [23,24].

We developed $CaCu_{3-x}Zn_xTi_{4-x}Ce_xO_{12}$ ceramics with x = 0.1, 0.2 and 0.3 through semi-wet growth method followed by auto-combustion at room temperature . This highlights the effect of Zn and Ce in CCTO ceramics on the dielectric properties and microstructure of this material. This approach for preparation of CCTO ceramics was used because of its reduced soaking time and lower sintering temperature compared to other conventional solid state reaction methods.

II. Experimental

The nanocrystalline $CaCu_{3-x}Zn_xTi_{4-x}Ce_xO_{12}$ (CCZTC-x) powders (where x = 0.1, 0.2 and 0.3, $CaCu_{2.9}Zn_{0.1}Ti_{3.9}Ce_{0.1}O_{12}$, $CaCu_{2.8}Zn_{0.2}Ti_{3.8}Ce_{0.2}O_{12}$ and $CaCu_{2.7}Zn_{0.3}Ti_{3.7}Ce_{0.3}O_{12}$) were synthesized via semi-wet growth using $Ca(NO_3)_2 \cdot 4\,H_2O$, $Cu(NO_3)_2 \cdot 3\,H_2O$, TiO_2 and citric acid as the starting materials. The metal nitrates were dissolved in doubly distilled water and aqueous solutions containing Ca^{2+}, Cu^{2+}, Zn^{2+} and Ce^{3+} were mixed in a beaker with stoichiometric amount of TiO_2. Then, citric acid (equivalent to metal ions) was added to the solutions. The resulting heterogeneous solutions were heated on a hot plate under stirring at 90–100 °C to vaporize the water and concede auto-combustion. The combustion occurred at room temperature and burnt under self-propagating reaction conditions, which released huge amount of gases and churn out the fluffy mass of $CaCu_{3-x}Zn_xTi_{4-x}Ce_xO_{12}$ (CCZTC-x) nanocrystalline powders. The nanocrystalline CCZTC-x powders were calcined in air at 800 °C for 8 h in an electrical furnace. The calcined CCZTC-x powders were mixed with 2 wt.% polyvinyl alcohol (PVA) and pressed at 4 MPa into cylindrical pellets using a hydraulic press. The PVA binder was burnt out at 350 °C for 2 h and the CCZTC-x pellets were finally sintered at 950 °C for 14 h.

The crystalline phases of the sintered samples were identified by using the X-ray diffraction (XRD) analysis (Rich-Siefert, ID-3000) employing CuKα radiation. The samples were scanned at 0.02 °/min over the 2θ range of 20–80°. The particle size and morphology were evaluated using a high-resolution transmission electron microscope (HR-TEM, FEI Tecnai F30). The analyses were prepared by dispersing the calcined CCZTC-x powders in acetone by ultra-sonication and deposited onto carbon-coated copper grids. The microstructural features of the fractured sintered ceramics were investigated using a scanning electron microscope (SEM, Model JEOL JSM5410).

The sintered pellets were polished using SiC abrasive paper and diamond paste until they had a mirror finish. For the purpose of the dielectric and electrical measurements, silver paste was applied to both sides of the circular surfaces of the ceramic pellets which were then dried at 600 °C for 15 min and cooled naturally to room temperature. The electric and dielectric properties of the CCZTC-x (x = 0.1, 0.2 and 0.3) ceramics were determined using LCR meter (PSM 1735, Newton4th Ltd, UK) over the frequency range of 10^2–10^6 Hz in the temperature range of 300–500 K.

III. Results and discussion

High resolution TEM and selected area diffraction (SAED) were used for examination of phase purity and crystallinity of the CCZTC-x powders. Figure 1a shows the bright filed TEM image of an agglomerated particle of the sample CCZTC-0.1. In Fig. 1b highly sym-

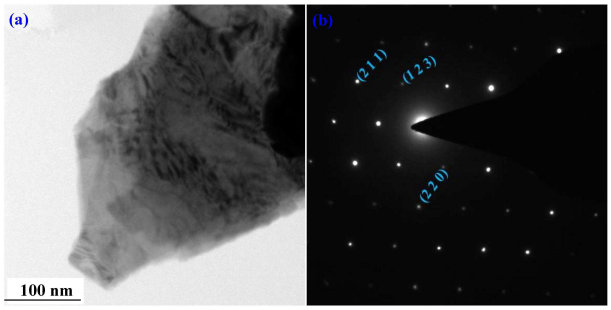

Figure 1. Bright field TEM image (a) and SAED pattern (b) of CCZTC-0.1 particle

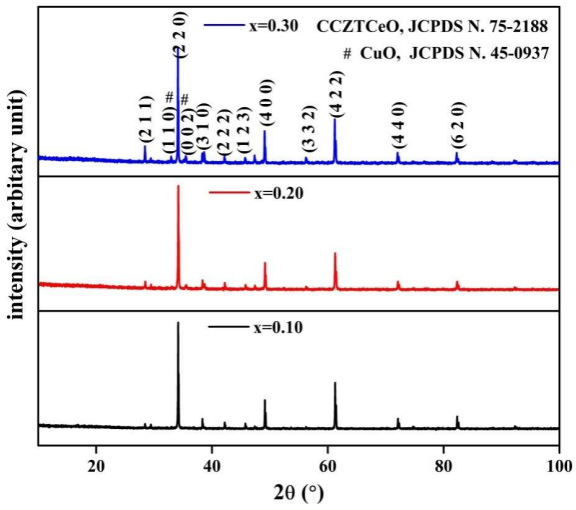

Figure 2. X-ray diffraction patterns of CCZTC-*x* ceramics sintered at 950 °C for 14 h in air

metrical dotted pattern is observed in the SAED which confirms the crystalline nature of the material.

Furthermore, SAED pattern has diffraction spots corresponding to the (211), (123) and (220) reflections, which correctly match with JCPDS Card No. 75-2188, confirming the cubic phase of the CCZTC-*x* powders and space group $Im\bar{3}$. The zone axes of the diffraction spots in between the plane (211) and (123), (123) and (220) are found to be $[1\bar{5}3]$ and $[\bar{6}6\bar{2}]$, respectively [25].

XRD analysis of the CCZTC-*x* ceramics sintered at 950 °C for 14 h in air are depicted in Fig. 2. The main CCTO phase (with $Im\bar{3}$ cubic symmetry) was confirmed together with some extra peaks of CuO as impurity phase. Present CCTO and CuO peaks in the CCZTC-*x* ceramics correspond to the standard data of JCPDS Cards No. 75-2188 and 45-0937, respectively. The intensity of CuO XRD peaks increases with increasing the dopant content. Therefore, the peaks of CuO are almost not observed in the case of the CCZTC-0.1 sample and very weak in the CCZTC-0.2 sample.

Figure 3a shows SEM micrographs of the CCZTC-*x* ceramics sintered at 950 °C for 14 h in air. Cubic-shaped grains are noticeable in the SEM micrographs, but they are not dominant in all compositions of CCZTC-*x* ceramics [26]. The average grain sizes of CCZTC-*x* ceramics were measured with ImageJ software and found to be 0.76, 0.87 and 0.98 μm for doping concentrations of x = 0.1, 0.2 and 0.3, respectively. From the above results, it is observed that calculated average grain size increases with increasing the concentrations of Zn and Ce in CCZTC-*x* ceramics [27]. At the same time, uniformity of grain size distribution decreases and some much larger CCTO grains can be seen in the sample CCZTC-0.3 ceramics (Fig. 3c).

Dielectric properties at different temperatures and frequencies were analysed by using high-precision multi-meters. Values of ε and $\tan\delta$ were calculated from capacitance data at measured temperatures and frequencies. The following general expression was used:

$$\varepsilon = \frac{C \cdot l}{\varepsilon_0 \cdot A} \tag{1}$$

where, ε and ε_0 are the dielectric permittivity and free space permittivity (8.85×10^{-12} F/m), and A, C and l are area of cylindrical pellets, capacitance and thickness of the pellets.

Figures 4a and 4b depict the frequency dependent trends of relative dielectric permittivity (ε_r) and tangent loss ($\tan\delta$) at 303 K of the CCZTC-*x* ceramics. Decreases in both the value of ε_r and $tan\delta$ are observed with increasing frequency until they become constant in higher frequency regions [28,29]. The values of ε_r and $\tan\delta$ at 100 Hz of the CCZTC-0.3 sample are 1500 and 32.2, respectively. The higher values of both ε_r and $\tan\delta$ at lower frequency are due to the semiconducting nature of grains surrounded by insulating grain boundaries. This causes interfacial charge polarization at the grain boundaries supported by internal barrier layer capacitance (IBLC) mechanism [30].

The change of ε_r and $\tan\delta$ of the prepared CCZTC-*x* ceramics with temperature at 10 kHz is shown in the Fig. 5. Values of ε_r and $\tan\delta$ increase with increasing dopant concentration and for the CCZTC-0.3 sample at 500 K are 314 and 4.7, respectively. The higher ε_r values at higher temperatures may arise from the difference of conductivity in the materials which enhance the space charge polarization [31].

The change of conductivity with frequency of the CCZTC-*x* ceramics at temperature of 303 K was also measured (Fig. 6). The total conductivity (σ) due to

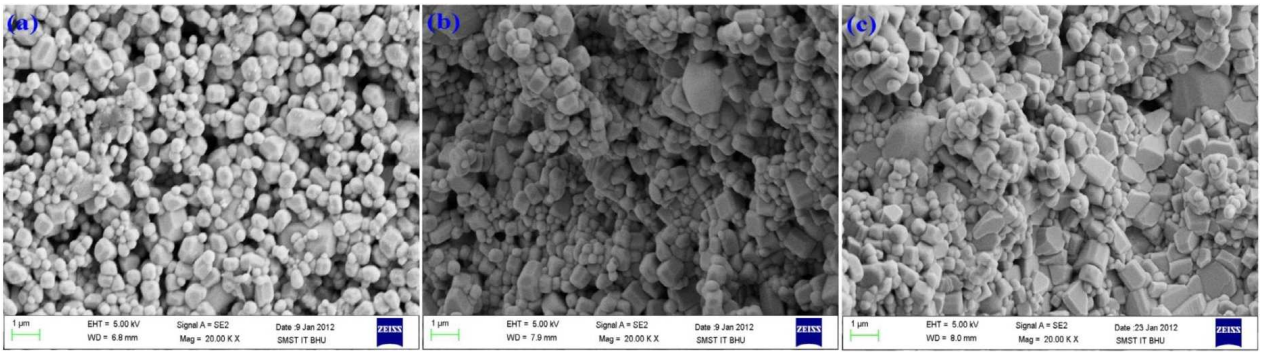

Figure 3. SEM micrographs of CCZTC-*x* ceramics: a) x = 0.1, b) x = 0.2 and c) x = 0.3

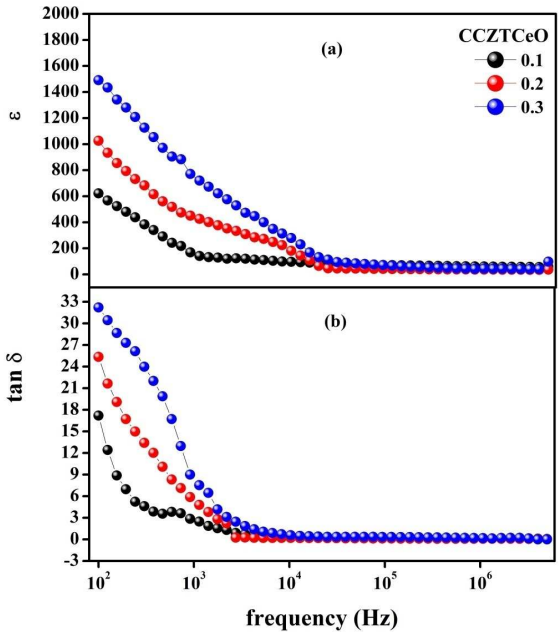

Figure 4. Frequency dependent dielectric constant, ε_r (a) and dielectric loss, tanδ (b) of CCZTC-x ceramics

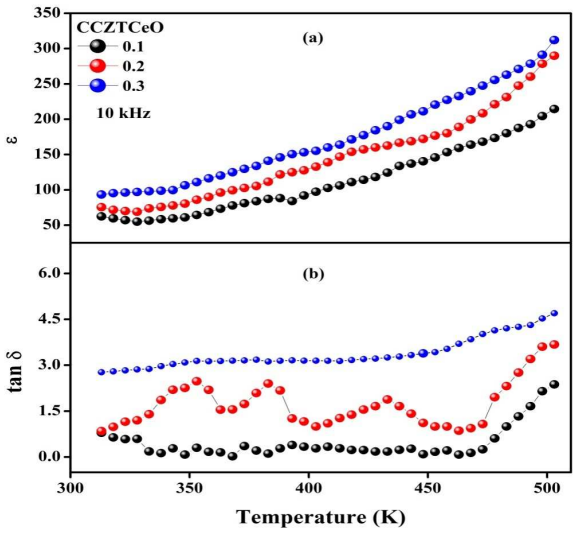

Figure 5. Temperature dependent dielectric constant, ε_r (a) and dielectric loss, tanδ (b) at 10 kHz of CCZTC-x ceramics

AC and DC contributions obeys the Almond-West type power law, expressed by following formula:

$$\sigma = \sigma_{DC} + \sigma_{AC} = \sigma_{DC} + A \cdot \omega^s \qquad (2)$$

The frequency dependent conductivity of material due to AC contribution follows the Jonscher's power law, given by the following expression:

$$\sigma_{AC} = A \cdot \omega^s \qquad (3)$$

where, A is the temperature dependent constant, ω is angular frequency and s frequency exponent term indicating the degree of interaction between mobile ions whose

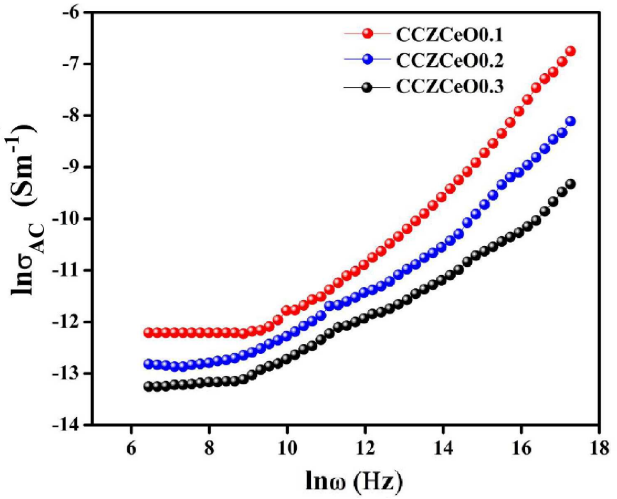

Figure 6. Plot of the AC conductivity (σ_{AC}) vs. frequency of CCZTC-x ceramics

value lies between 0 and 1 and it depends both on temperature and concentrations of mobile ions. Lower value of s represents the frequency independence of electrical conduction and its higher value (s = 1) represents frequency dependent conductivity.

From Fig. 6 a flat response of conductivity is observed in the lower frequency region for all compositions which may be due to the DC contribution of conductivity (σ_{DC}). Rapid increase of conductivity is obvious at higher frequencies. The values of exponent s, calculated by plotting $\ln \sigma_{AC}$ vs. $\ln \omega$, are 0.811, 0.792 and 0.773 for the samples with x = 0.1, 0.2 and 0.3, respectively. The decreasing value of s with increasing concentration obtained by linear fitting may be due to the hopping charge conduction mechanism.

Figure 7 depicts the AC conductivity plots versus inverse temperature ($\ln \sigma_{AC}$ vs. $1/T$) performed at 10 kHz for the CCZTC-x ceramics. The temperature dependence of AC conductivity defined by the Arrhenius law is expressed by the following relation:

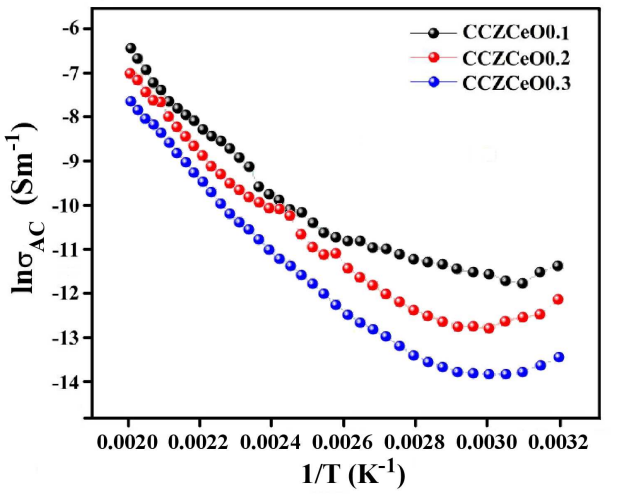

Figure 7. Plot of the AC conductivity (σ_{AC}) vs. temperature of CCZTC-x ceramics

$$\sigma = \sigma_0 \cdot \exp\left(-\frac{E_a}{k \cdot T}\right) \quad (4)$$

where, σ_0 pre-exponential factor, E_a is the activation energy for ionic conduction, k is the Boltzmann constant and T is the absolute temperature. The activation energies of the CCZC-0.1, CCZTC-0.2 and CCZTC-0.3 ceramics were calculated from the slope of the $\ln \sigma_{AC}$ vs. $1/T$ curve and obtained values were 0.93, 0.76 and 0.74 eV, respectively. The lower activation energy values of the CCZTC-0.2 and CCZTC-0.3 ceramics indicate on their more conducting nature than for the lowest dopant composition. Lower conductivity values of the CCZTC-0.3 are correlated to high space charge polarization at the grain boundary regions which enhances its dielectric constant.

Ferroelectric properties of the CCZTC-x ceramics were investigated by measuring polarization versus electric field (P-E hysteresis loop) at room temperature and operating frequency 50 Hz under the application of applied electric field up to 4.8 kV/cm (Fig. 8). The absence of saturation in the P-E hysteresis loop is most probably due to the low applied electric field and the loosely behaviour of the CCZTC-x ceramics [32]. Furthermore, improper hysteresis loop of banana type is apparent and might result from both domain switching and electric conductivity contributions [33]. However, the decrease in remnant polarization (P_r) and increase in coercivity (E_c) with the increase of dopant concentration are obvious. The calculated P_r and E_c values of the samples with x = 0.1, 0.2 and 0.3 are 0.0042, 0.0047, 0.0058 μC/cm^2 and 0.645 0.421, 0.354 kV/cm, respectively. The observed change of P_r and E_c might be correlated to grain size effect [34].

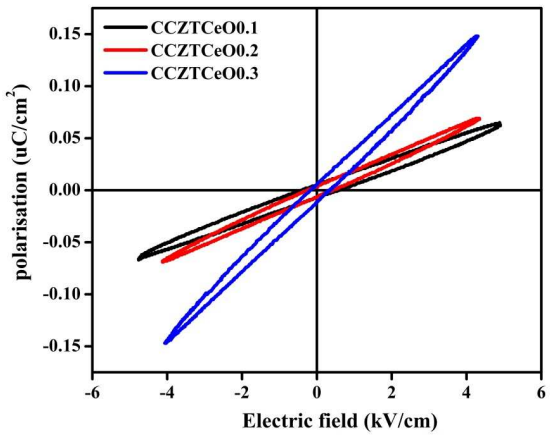

Figure 8. Plot of polarization versus electric field (*P-E* hysteresis loop) at 50 Hz of CCZTC-*x* ceramics for *x* = 0.1, 0.2 and 0.3

IV. Conclusions

$CaCu_{3-x}Zn_xTi_{4-x}Ce_xO_{12}$ (x = 0.1, 0.2 and 0.3) ceramics were fabricated by semi-wet growth route and sintering at 950 °C. The presence of major CCTO phase along with the minor CuO phase was confirmed by XRD analysis. Cubical shape grains have been seen in SEM micrographs for all selected compositions and the average grain sizes were 0.76, 0.87 and 0.98 μm for the samples with x = 0.1, 0.2, 0.3, respectively. Conductivity of the sintered samples decreases with doping concentration and values of dielectric permittivity and tangent loss at lower frequency are observed to be 1500 and 32.2, respectively. P-E hysteresis curve shows loose behaviour due to the absence of saturation. Although, the dielectric constant of the present materials is not too high, it is found that the bi-substitution in CCTO enhances the ferroelectric properties.

Acknowledgements: Dr. Laxman Singh is grateful to the concerned authorities of Siddharth University and those of extending support to prepare this manuscript.

References

1. J. Zhang, Y. Q. Li, Q. Yang, Y. Yang, F. Meng, T. Wang, Z. Xia, Y. Wang, K. Chen, Q. Zhang, L. Gu, J. Liu, J. Zhu, "A structural perspective on giant permittivity $CaCu_3Ti_4O_{12}$: One way to quantum dielectric physics in solids", *Open Ceram.*, **6** (2021) 100126.
2. L. Marchin, S. Guillemet-Fritsch, B.Durand, A.A. Levchenko, A. Navrotsky, T. Lebey, "Grain growth- controlled giant permittivity in soft chemistry $CaCu_3Ti_4O_{12}$ ceramic", *J. Am. Ceram. Soc.*, **91** [2] (2008) 485–489.
3. Y. Li, W. Li, G. Du, N. Chen, "Low temperature preparation of $CaCu_3Ti_4O_{12}$ ceramics with high permittivity and low dielectric loss", *Ceram. Int.*, **43** (2017) 9178–9183.
4. C. Mao, L. Xu, V.V. Marchenkov, T.V. Dyachkova, A.P. Tyutyunnik, Y.G. Zainulin, C. Yang, "Microstructure and dielectric properties of $CaCu_3Ti_4O_{12}$ ceramics by quenching after sintering in low vacuum and thermobaric treatment at 9 GPa", *Ceram. Int.*, **44** (2018) 20069–20074.
5. R. Schmidt, M.C. Stennett, N.C. Hyatt, J. Pokorny, J. Parado-Gonjal, M. Li, D.C. Sinclair, "Effects of sintering temperature on the internal barrier layer capacitor (IBLC) structure in $CaCu_3Ti_4O_{12}$ (CCTO) ceramics", *J. Eur. Ceram. Soc.*, **32** (2012) 3313–3323.
6. A.P. Kajal, P. Kumar, "Giant dielectric properties of $CaCu_3Ti_4O_{12}$ ceramics synthesized by solid state reaction route", *Process. Appl. Ceram.*, **17** [4] (2023) 393–399.
7. J. Li, M.A. Subramanian, H.D. Rosenfeld, C.Y. Jones, B.H. Toby, A.W. Sleight, "Clues to the giant dielectric constant of $CaCu_3Ti_4O_{12}$ in the defect structure of "$SrCu_3Ti_4O_{12}$"", *Chem. Mater.*, **16** (2004)5223–5225.
8. T.B. Adams, D.C. Sinclair, A.R. West, "Decomposition reactions in $CaCu_3Ti_4O_{12}$ ceramics", *J. Am. Ceram. Soc.*, **89** (2006) 2833.
9. Y. Li, P. Liang, X. Chao, Z. Yang, "Preparation of $CaCu_3Ti_4O_{12}$ ceramic with low dielectric loss and giant dielectric constant by sol-gel technique", *Ceram. Int.*, **39** (2013) 7879–7889.
10. M.-H. Wang, B. Zhang, F. Zhou, "Preparation and characterization of $CaCu_3Ti_4O_{12}$ powder by non-hydrolytic sol-gel method", *J. Sol-Gel Sci. Technol.*, **70** (2014) 62–66.
11. J. Liu, R.W. Smith, W.N. Mei, "Synthesis of giant dielectric constant material $CaCu_3Ti_4O_{12}$ by wet chemistry

methods", *Chem. Mater*., **19** (2007) 6020–6024.
12. S. Babu, A. Govindan, "Dielectric properties of $CaCu_3Ti_4O_{12}$ (CCTO) prepared by modified solid- state reaction method", *Inter. Rev. Appl. Eng. Res.*, **4** (2014) 275–280.
13. A. Gendanken, "Sonochemistry and its application to nanochemistry", *Curr. Sci*., **85** (2003) 1720–1722.
14. P. Mao, J. Wang, S. Liu, L. Zhang, L. Zhao, L. He, "Grain size effect on the dielectric and non-ohmic properties of $CaCu_3Ti_4O_{12}$ ceramics prepared by the sol-gel process", *J. Alloys Compd*., **778** (2019) 625–632.
15. L. Singh, I.W. Kim, B.C. Sin, A. Ullah, S.K. Woo, Y. Lee, "Study of dielectric, AC-impedance, modulus properties of $0.5Bi_{0.5}Na_{0.5}TiO_3$-$0.5CaCu_3Ti_4O_{12}$ nano-composite synthesized by a modified solid state method", **31** (2015) 386–396.
16. M.A. Ramirez, P.R. Bueno, J.A. Varela , E. Longo, "Non-ohmic and dielectric properties of $CaCu_3Ti_4O_{12}$ polycrystalline of system", *Appl. Phys. Lett*., **89** (2006) 212102.
17. Z. Yang, Y. Zhang, Z.H. Lu, K. Zhang, R. Xiong, J. Shi, "Electrical conduction and dielectric properties of the Rb-doped $CaCu_3Ti_4O_{12}$", *J. Am. Ceram. Soc*., **96** (2013) 806–811.
18. K. Nurmi, H. Jantunen, J. Juuti, "The impact of lanthanum doping on the microstructure and colossal permittivity in $Ba_xSr_{(1-x)}TiO_3$", *Open Ceram.*, **6** (2021) 100120.
19. S.W. Choi, Y.M. Kim, S.H. Hong, "Effect of Al doping on the electric and dielectric properties of $CaCu_3Ti_4O_{12}$", *J. Am. Ceram. Soc*., **90** (2004) 4009–4011.
20. R. Kashyap, O.P. Thakur, R.P. Tandon, "Study of structural, dielectric and electrical conduction behaviour of Gd substituted $CaCu_3Ti_4O_{12}$ ceramic", *Ceram. Int.*, **38**, (2012) 3029–3037.
21. L. Singh, B.C. Sin, I.W. Kim, K.D. Mandal, H. Chung, Y. Lee, J. Varela, "A novel one step flam synthesis method for tungsten-doped CCTO ceramic", *J. Am. Ceram. Soc*., **99** (2016) 27–34.
22. J. Boonakhorn, P. Thongboi, B. Putasaeng, T. Yamwong, S. Maensiri, "Very high-performance dielectric properties of $Ca_{1-3x/2}Yb_xCu_3Ti_4O_{12}$ ceramic", *J. Alloys Compd*., **612** (2014) 103–109.
23. M. Li, X.L. Chen, D.F. Zhang, W.Y. Wang, W.J. Wang, "Humidity sensitive properties of pure and Mg-doped $CaCu_3Ti_4O_{12}$", *Sensor. Actuat. B Chem.*, **147** (2010) 447–452.
24. D. Xu, C. Zhang, X.N. Cheng, Y. Fan, T. Yang, H.M. Yuan, "Dielectric properties of Zn-doped CCTO ceramics by sol-gel method", *Adv. Mater. Res*., **197** (2011) 302–305.
25. L. Singh, U.P. Azad, S.P. Singh, V. Ganesan, U.S. Rai, Y. Lee, "Yttrium copper titanate as a highly efficient eletrocatalyst for oxygen reduction reaction in fuel cell, synthesized via ultrafast automatic flame technique", *Sci. Report*, **7** (2017) 9407.
26. P. Thiruramanathan, A. Marikani, S. Ravi, D. Madhavan, G.S. Hikku, "Fabrication of miniaturized high band width dielectric resonator on patch (DRoP) antenna using high dielectric $CaCu_3Ti_4O_{12}$ nanoparticles", *J. Alloys Compd*., **747** (2018) 1033–1042.
27. L. Singh, U.S. Rai, K.D. Mandal, "Influence of Zn doping on microstructures and dielectric properties in $CaCu_3Ti_4O_{12}$ ceramic synthesised by semiwet route", *Adv. Appl. Ceram*., **111** [7] (2012) 374–380.
28. L. Singh, U.S. Rai, A.K. Rai, K.D. Mandal, "Sintering Effects on dielectric properties of Zn-doped $CaCu_3Ti_4O_{12}$ ceramic synthesized by modified sol-gel route", *Electron. Mater. Lett*., **9** [1] (2013) 107–113.
29. L. Singh, U.S. Rai, A.K. Rai, K.D. Mandal, "Dielectric behavior of $CaCu_3Ti_4O_{12}$ electro-ceramic doped with La, Mn and Ni synthesized by modified citrate-gel route", *J. Adv. Ceram*., **2** [2] (2013) 119–127.
30. L. Singh, S.S. Yadava, W.S. Woo, U.S. Rai, K.D. Mandal, B.C. Sin, Y. Lee, "Structural, impedance, and modulus spectroscopic studies on $Y_{2/3}Cu_3Ti_{3.95}In_{0.05}O_{12}$ polycrystalline material prepared by flame synthesis method", *Appl. Spectrosc. Rev.*, **51** (2016) 735–752.
31. L. Singh, U.S. Rai, K.D. Mandal, B.C. Sin, S.I. Lee, Y. Lee, "Dielectric, AC-impedance, modulus studies on $0.5BaTiO_3 \cdot 0.5CaCu_3Ti_4O_{12}$ nano-composite ceramic synthesized by one-pot, glycine-assisted nitrate-gel route", *Ceram. Int*., **40** (2014) 10073–10083.
32. A. Kumar, M.K. Verma, S. Singh, T. Das, L. Singh, K.D. Mandal, "Electrical, magnetic and dielectric properties of cobalt-doped barium hexaferrite $BaFe_{12-x}Co_xO_{19}$ (x = 0.0, 0.05, 0.1 and 0.2) ceramic prepared via a chemical route", *J. Electron. Mater*., **49** (2020) 6436–6447.
33. M. Dawber, K.M. Rabe, J.F. Scott, "Physics of thin-film ferroelectric oxides", *Rev. Modern Phys.*, **77** [4] (2005) 1083–1130.
34. A.R Tanna, H.H. Josh, "Effect of high energy mechanical milling on hysteresis and dielectric properties of $Ca_xBa_{1-x}Zr_xTi_{1-x}O_3$ (x = 0 and 0.1) ferroelectric materials", *Mater. Res. Express*, **5** (2018) 096302.